SPECTROSCOPIC IMAGING TECHNIQUES FOR DETECTING CALCIFICATION IN THE KNEE JOINT TISSUE

University of Oulu
Study program of Physics,
Biomedical physics
Bachelor thesis, Spring 2022
Reeta Nissinen

Table of contents

1. Introduction

Osteoarthritis (OA) is the most common form of arthritis that is costly both economically and socially[1]. Since OA is irreversible, researchers are constantly seeking the most efficient and reliable method of diagnosing it at an early stage. OA is closely associated with the development of calcifications in soft tissues of the knee joint, such as the meniscus and articular cartilage (AC). These crystal-induced calcifications may represent a potential target for disease-modifying agents in OA treatment. The presence of OA-associated crystals can be also found in the synovial fluid (SF). Among the most common types of crystals found to be associated with OA are basic calcium phosphate (BCP) and calcium phosphate dihydrate (CPPD)[2]. Although BCP and CPPD crystals may coexist, their clinical patterns and etiology differ significantly[3]. The detection and characterization of OA-related crystals are challenging since they have sub-micron structures, and they can coexist with other crystal deposition disorders like pseudogout or gout. OA-related changes in AC and SF have been extensively studied, in addition, in recent years the meniscus has also been taken into consideration. It has been reported that the meniscus can be calcified even though the AC is not[2]. According to these results, meniscal calcification may potentially be a risk factor for cartilage lesions. There are a number of analytical techniques that have been applied to detect and characterize crystals in knee joint tissue, either directly or indirectly. This thesis focuses on different spectroscopic techniques available for detecting calcium crystals in synovial fluid, articular cartilage, and meniscus of the knee joint. Particularly, this thesis aims to systematically review the spectroscopic studies related to the detection of calcification from knee join tissue and presents an experiment that characterizes calcifications in meniscus using Raman spectroscopy.

2. Anatomy of knee joint

2.1 Synovial fluid

Synovial fluid is a viscous liquid found within the synovial cavities (Fig. 1). It is formed when blood plasma is filtered into the synovial cavities through the synovial membrane[4]. Along with the proteins in the blood plasma, SF also includes molecules, such as hyaluronan (HA), proteoglycan 4 (PRG4), also known as lubricin, and surface-active phospholipids (SAPL) produced by chondrocytes in articular cartilage, synoviocytes in the synovial membrane and meniscus[4]. HA and PRG4 contribute to making SF viscous and, consequently, to making it work as a lubricant in the knee joint[4]. It is yet unclear whether SAPL plays a role in joint lubrication[4]. The lubrication properties of SF reduce friction between opposing surfaces of AC; hence, it protects AC in joints[5]. Additionally,

SF also serves as a nutrient and metabolic waste transporter between the synovial membrane and AC[4,5].

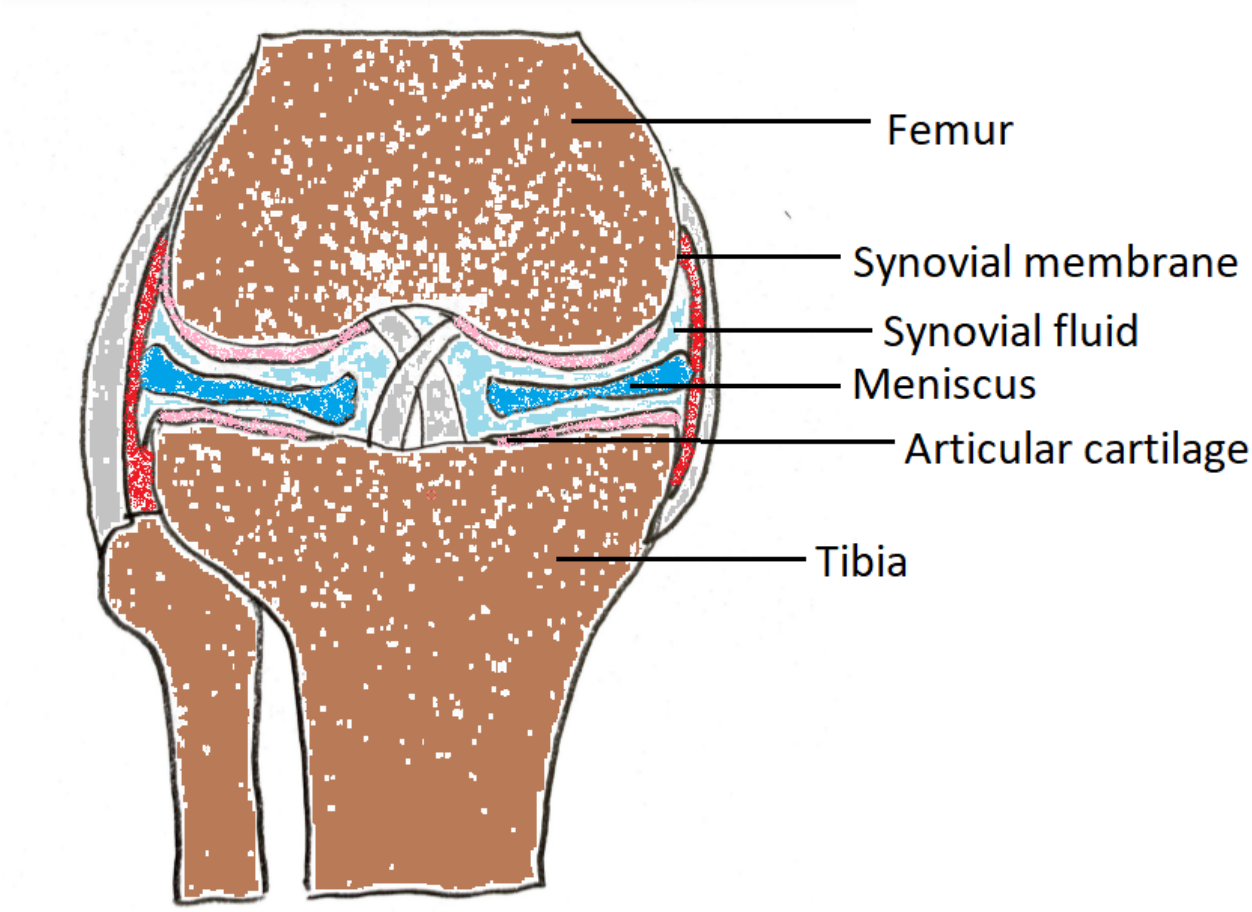

Fig 1: Front view of the anatomy of the human knee joint. Articular cartilage is covering the end of the femur and tibia. Menisci are attached to joints on the sides, and it lies between the bones surrounded by synovial fluid which fills the joint cavity.

2.2 Articular cartilage

Articular cartilage is hyaline cartilage that covers the end of long bones, femur, and tibia, in the knee joint (Fig.1). It is composed of a dense extracellular matrix (ECM) and chondrocytes. The ECM consists mainly of water, type II collagen, and proteoglycans[6]. There are also some non-collagenous proteins and glycoproteins present[6]. These components work together to maintain the mechanical properties of the ECM by retaining water within it[6]. Articular cartilage is avascular and the lymphatics, as well as nerves, are absent. Therefore, nutrients and oxygen are delivered to cells through the SF, resulting in a limited ability to repair itself[7].

Articular cartilage can be classified into four groups: superficial zone, middle zone, deep zone, and calcified zone[6](Fig. 2). The superficial zone, which is in contact with synovial fluid, makes up approximately 10 % of AC and protects deeper layers by resisting the tensile and compressive

forces of joint movement[6]. In this zone, collagen fibers run parallel to the surface of articular cartilage, and chondrocytes are mostly flattened. The zone between the superficial and deep zone is the middle zone, which provides an anatomical and functional bridge between those two. Additionally, the middle zone resists compression forces to some extent. Approximately 40% to 60% of the articular cartilage consists of the middle layer[6]. It contains proteoglycans and spherical chondrocytes at low density. In this layer, the collagen fibers are thick and obliquely organized. The deep zone, in turn, provides the greatest resistance to compression forces. The deep zone makes up approximately 30 % of the articular cartilage volume[6]. In the deep zone, the proteoglycan content is the greatest, and collagen fibers are the thickest and arranged vertically to the articular surface. In addition, the water concentration is the lowest. The chondrocytes are generally arranged along collagen fibers in a columnar arrangement. Beneath the deep zone, there is the calcified zone, which attaches the cartilage to the bone.

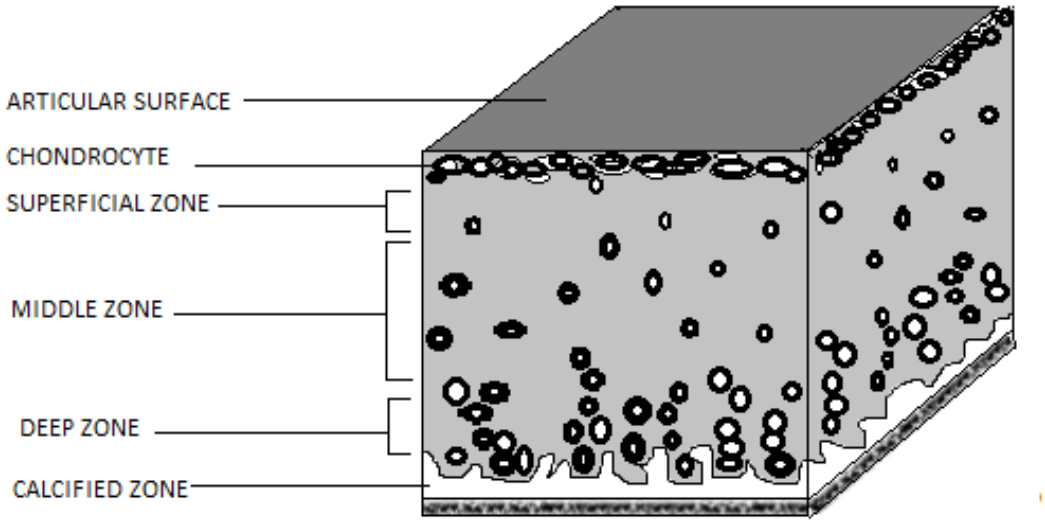

Fig 2: A schematic presentation of the cross-section of articular cartilage in healthy articular cartilage presenting three non-calcified zones superficial, middle, and deep, as well as the chondrocytes within those. The calcified zone beneath attaches the articular cartilage to the bone.

In general, articular cartilage's primary purpose is to provide a smooth and lubricated surface, which is necessary for minimizing friction. In the knee joint, it functions as a shock absorber by aiding the transmission of loads to the subchondral bone underneath[6].

2.3 Meniscus

The meniscus is a wedge-shaped fibrocartilaginous tissue (Fig 3). Its outer peripheral surfaces are thick, vascularized, and attached to the joint. Inner borders are thin and unattached to the joint.

The meniscus is quite an exceptional cartilage as it has its own blood supply, and it is internally innervated. It consists of a large ECM which is composed mainly of water (72 %) and collagen fibers (22 %)[8]. Proteoglycans, elastin, and other glycoproteins make up the rest of the ECM[8]. Most of the collagen fibers in the meniscus are Type I collagen, although Type II-IV are also found[8]. It is the collagens that are responsible for forming the fibrocartilage network of a meniscus. The meniscus can be divided into three different cross-sections, with different type I collagen fiber organizations[9]. In the superficial network, thin collagens form a meshwork, which covers the surface of the meniscus[9]. Beneath the superficial layer is a lamellar layer. In the lamellar layer, the collagen fibers are orientated in the radial direction[9]. Most of the collagen fibers are in the central main layer, where they are oriented circularly[9]. This structure is optimal for transmitting vertical compression loads to circumferential hoop stresses[8].

In the human knee, there are two menisci: lateral and medial; both of which are located between the femur and the tibia. They can be considered as extensions of the tibia since there are firmly attached to it through anterior and posterior horns which continue as external ligaments[10]. A transverse ligament connects the menisci, which enables these structures to function as one unit[8].

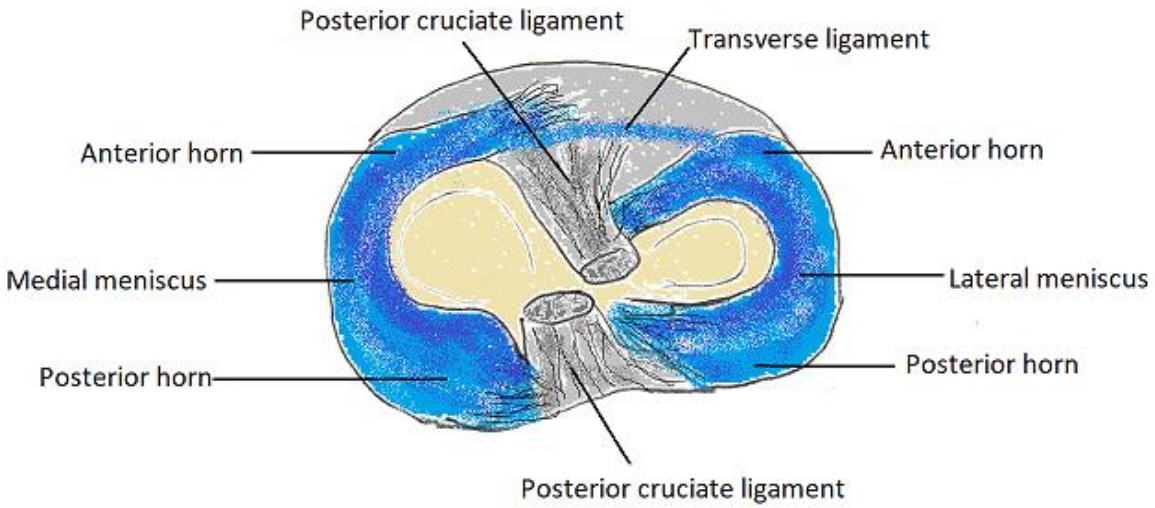

Fig 3: Top view of the anatomical human meniscus. Wedge-shaped menisci are attached to posterior and anterior horns that continue as posterior and anterior ligaments. The transverse ligament between the menisci connects them to each other, enabling them to work as a unit.

The meniscus functions primarily as a force transmission and shock absorber[8]. However, it also plays a part in the improvement of knee joint stability and in providing frictionless movement by compressing synovial fluid into the articular cartilage[8].

3. Pathological calcification

3.1 In articular cartilage and synovial fluid

Two of the most common crystal types associated with knee joint disorders are basic calcium phosphate (BCP) and calcium phosphate dihydrate (CPPD)[2] (Table 1). However, it is yet uncertain from where these crystals originate, and whether these crystals are a cause or a consequence of the issues[3].

Table 1: Dimensions of the most common crystal types[3].

Crystals	Size
Basic calcium phosphate (BCP)	1nm (individual) 5-20µm(clumps)
Calcium pyrophosphate dihydrate (CPPD)	1-20µm

According to several studies, BCP crystals appear to play a crucial role in articular cartilage degeneration in OA, and if found, they can assist in diagnosis[3]. One of the ways to diagnose OA is currently considered to be to identify the common types of crystals associated with it in synovial fluid[3]. SF can become supersaturated with BCP due to BCP crystals' low solubility in it[3]. Approximately 60 % of synovial fluid samples from people with OA contain BCP crystals[3]. As BCP crystals are currently difficult to detect due to their sub-micron size, the complexity of synovial fluid, and the fact that they can co-exist with bigger CPPD crystals, it is likely that the percentage is even higher. Arthritic knees with BCP crystals have been reported to be more effused than arthritic knees without BCP crystals[2]. Additionally, crystals cause mechanical abrasion, which may aggravate the issues.

Recent studies show that OA articular cartilage is predominantly composed of the BCP crystals[2]. It has been reported that the concentration of BCP crystals in the synovial fluid increases with the severity of the OA[3]. It is considered that cartilage mineralization caused by BCP crystals is a progressive pathogenic factor in OA development.

3.2 In meniscus

A diagnosis of pseudogout, also known as CPPD crystal deposition disease is associated with meniscal calcification in 86 % of patients[2]. Additionally, meniscal calcification also tends to be more common with age[2]. Researchers have reported meniscal calcification even if the articular cartilage is not calcified[2]. Nevertheless, calcification of articular cartilage results in calcification of

the meniscus as well[2]. On the basis of reference (Sun & Mauerhan 2012)[2] Mitrovic et al. (1988) report that 80 % of elderly patients with calcified meniscus develop cartilage lesions as well, as opposed to only 35 % of those without calcification[2]. The results suggest that meniscal calcification may potentially predispose to cartilage lesions. The edges of diseased menisci are typically characterized by the presence of medium-sized and large BCP crystals. As joints move, meniscal minerals are released into the synovial fluid at the degenerative edges. Osteoarthritic meniscal cells appear to produce higher levels of minerals in synovial fluid than healthy ones[2]. Furthermore, OA knees show decreased cellularity, diffuse hypercellularity, and a hypertrophied meniscus. This suggests that calcification of the meniscus and articular cartilage may play a pathogenic role in OA.

4. Imaging methods

4.1 Fourier transform infrared spectroscopy

Fourier transforms infrared (FTIR) spectroscopy uses electromagnetic radiation in the wavelength range of infrared (IR) radiation to study a sample. The energy of the IR radiation can be calculated as the following:

$$E = hv = \frac{hc}{\lambda} \qquad \text{(Eq.1)}$$

where h is Planck's constant, v is the frequency of incident radiation, c is the speed of light in vacuum, and λ is the wavelength.

In the FTIR, the absorbed radiation causes the bonds between the molecules to vibrate. However, vibration absorbs the IR radiation only if the molecule changes its dipole moment during the vibration. Stronger the dipole moments cause more absorption. Thus, the IR spectrum does not detect symmetrical molecules such as N_2 and O_2, as they do not have a dipole moment. The IR absorption frequency depends on the bonding nature, reactions with the environment, and the relative masses of the atoms [11]. In FTIR spectroscopy wavelengths convertibly convert to wavenumbers $\bar{v}$, which is defined as:

$$\bar{v} = \frac{1}{\lambda} = \frac{v}{c} \qquad \text{(Eq.2)}$$

There are four main components of a modern FTIR spectrometer, which are (1) radiation source, (2) beam splitter, (3) mirrors, and the (4) detector (Fig. 4) [12]. When the radiation source is heated, IR radiation is generated. A semi-reflecting film is used as the beam splitter which reflects half of the generated radiation into a moving mirror and the other half into a static mirror. Both mirrors

reflect the radiation back at the beam splitter. The reflected radiations experience interference forming a united beam which is passed through the sample all the way to the detector called interferogram[13]. Using the Fourier transform, the computer works backward to determine what wavelengths each bond has absorbed and forms an infrared spectrum from the interferogram. On the infrared spectrum, the vibrations of the different bonds are commonly displayed as absorption spikes at the corresponding wavenumber. In FTIR spectroscopy, a microscope is combined with the FTIR spectrometer. This allows to view and focus the area of the sample to be analyzed and spatially map the sample at microscale resolution.

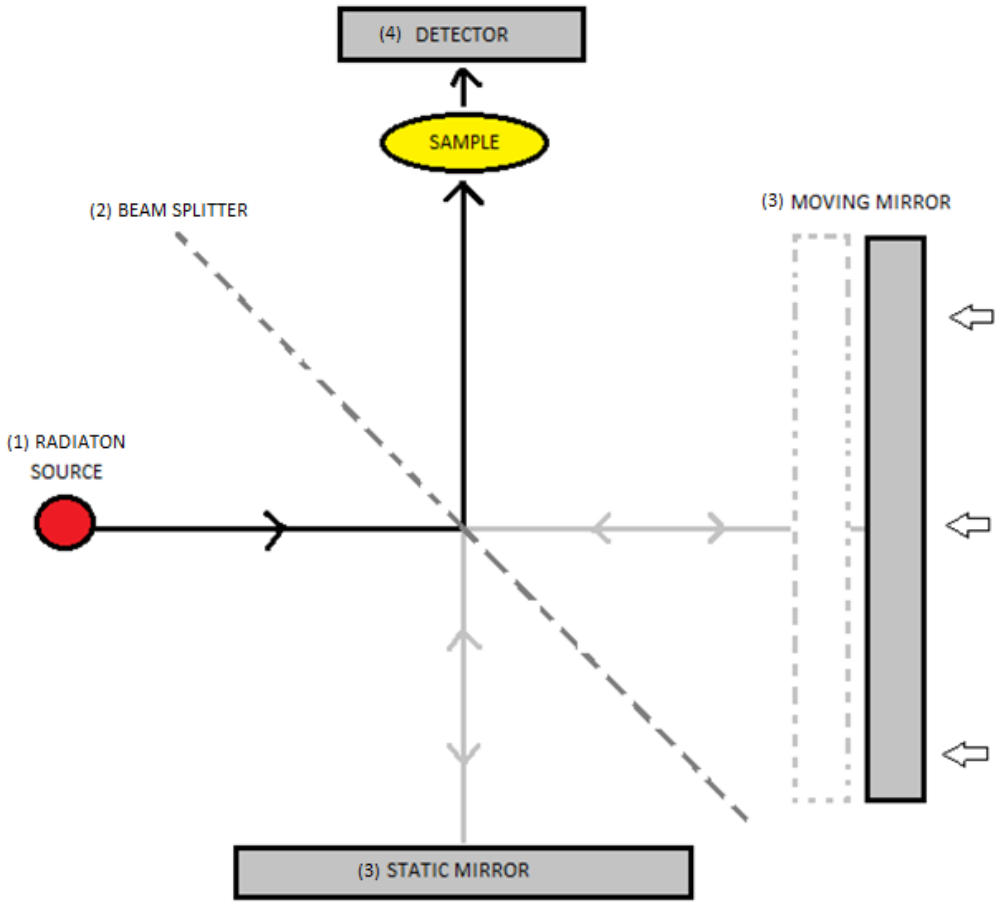

Fig 4: Schematic of FTIR spectrometer presenting basic components including a radiation source, beam splitter, two mirrors, and the detector behind the sample.

FTIR measurement techniques have a wide application range, including the analysis of small molecules or molecular complexes and the analysis of cells or tissues[11]. One of the major advantages of the FTIR measurement techniques is that it is fast, and the device is usually pre-automated allowing it to run mostly user-independently. FTIR is not interfered with by the fluorescence and the FTIR analysis can be done in any physical state of the sample. However, the

sample preparation is more time-consuming than measuring with a Raman spectroscope since water interferes with the IR measurement.

4.2 Raman spectroscopy

The Raman effect is the change of wavelength that occurs when a monochromatic light beam, such as a laser, is scattered by molecules. More specifically, as a beam of light passes through a sample, some of the light scatters in directions other than that of the incident beam. Most of this scattered light has the same wavelength as the incident beam of light. However, a small fraction of the scattered light has wavelengths different from that of the incident light. These different wavelengths are due to a Raman effect, which was discovered by Indian physicist C.V. Raman in 1928.

Raman spectroscopy is based on a study of the Raman effect. Raman spectroscopy allows the determination of the materials based on their spectrum since every material has its unique spectrum, which is like a fingerprint. By comparing the spectrum obtained from the material with what has previously been obtained from other known materials, the studied one can be identified. In addition, analysis of the spectrum can offer insights into the properties of the material, in which case if there are no previous equivalents.

In Raman spectroscopy, the scattering most commonly occurs in an elastic manner, known as Rayleigh's scattering. In Rayleigh's scattering, the wavelength of the scattered photons does not change (Fig. 5). In inelastic scattering, however, the wavelength of the scattered photons changes through Stokes or anti-Stokes Raman scattering (Fig.5). In Stokes Raman scattering, photons interact with the molecules so that the energy of the scattered photons shifts down. In Anti-Stokes Raman scattering, on the contrary, the energy of the scattered photons shifts up. During the Raman effect, the molecule system temporarily transfers to a higher energy level, a so-called virtual state. After a short while, the system returns either to a lower energy state or a ground state which depends on the type of scattering. Due to this energy shift, i.e., Raman shift, a photon whose wavenumber is the same as the energy difference of the two states is released. The energy of the inelastic Raman scattering is expressed as:

$$E = hc\bar{\nu} = hc(\bar{\nu}_0 \pm \bar{\nu}_M) \qquad \text{(Eq. 3)}$$

where $\bar{\nu}_0$ is the wavenumber of the incident photon and $\bar{\nu}_M$ is the wavenumber of the scattered photon. In Stokes Raman scattering the wavenumber of scattered photon $\bar{\nu}_M$ is positive, and in Anti-Stokes Raman scattering it is vice versa negative.

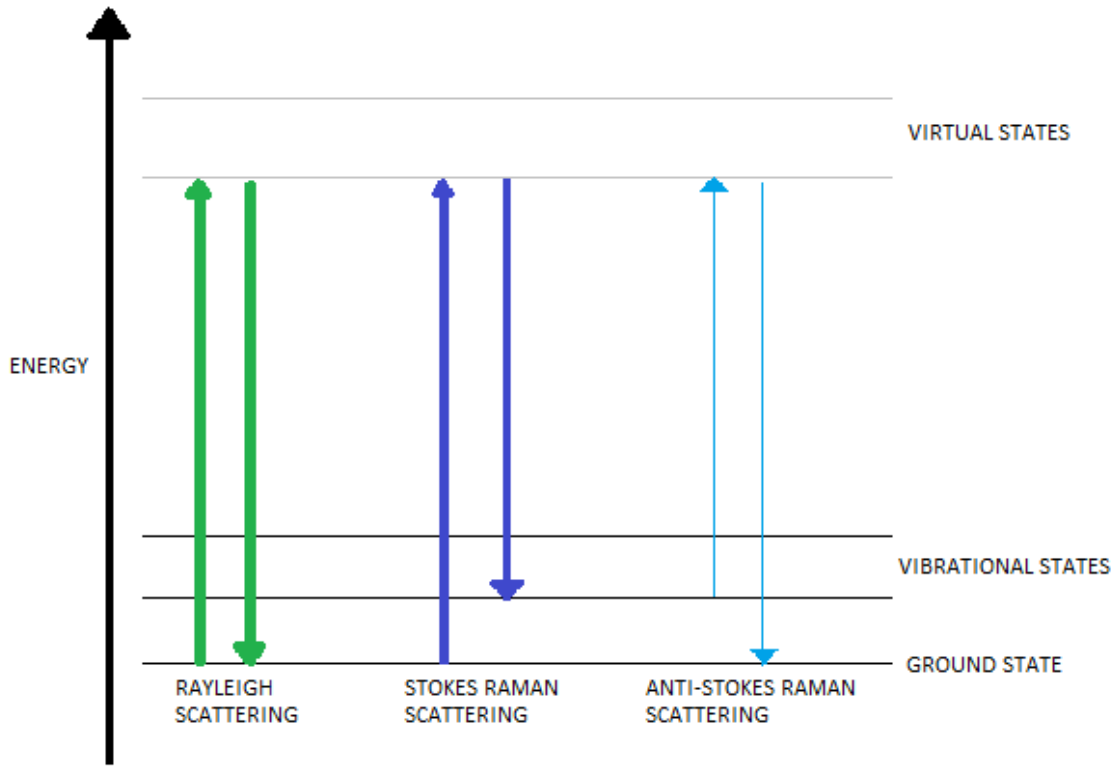

Fig 5: Energy level diagram of Rayleigh, Stokes Raman, and Anti-Stokes Raman scatterings. Arrows present how photons transit between ground-, vibrational-, and virtual states during scattering.

Stokes scattering which occurs from the ground state is stronger than the anti-stokes occurring from the higher vibration state, as Boltzmann's distribution suggests that the lower the energy states have more molecules. The strongest is Rayleigh scattering and it often covers up Raman scattering, which is why equipment is designed to filter the Rayleigh scattering out.

The Raman spectrometer consists of a laser source that is focused through an objective on a sample with the aid of an optical microscope (Fig.6). The sample lies on a motorized stage under the microscope, which enables sample movement. As the light scatters from the sample, it is collected by the same objective and filtered with a notch filter to remove Rayleigh's scattered photons. The Raman scattered photons are then collected with a multichannel two-dimensional charge-coupled device (CCD). After the CCD data is collected, it is electronically processed to form the Raman spectrum. In addition, in order to achieve optimal results, some instruments allow the user to select the laser wavelength and power.

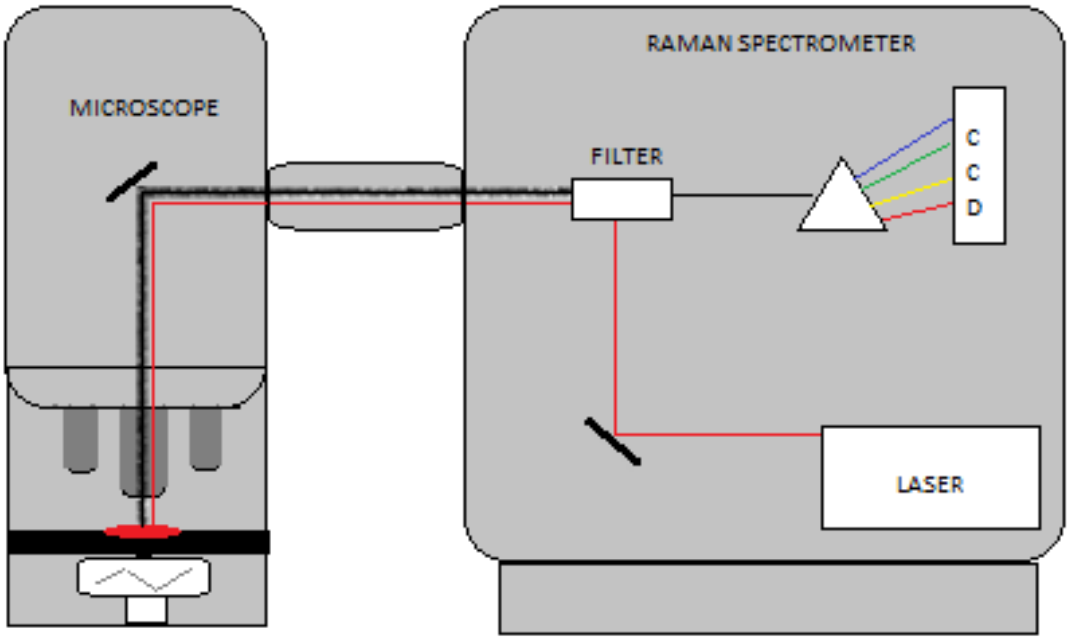

Fig 6: Schematic of Raman spectrometer presenting basic components including microscope with a movable stage and the Raman spectrometer with a laser source, filter for Rayleigh scattering, and CCD.

Raman spectroscopy has the advantage that very precise information can be obtained at the molecular level, and the water in the sample has only a minimal impact on the results. Thus, it is possible to study fresh tissues and water solutions, such as synovial fluid[3]. A disadvantage of the device is its high price and the presence of background fluorescence in biological samples. Additionally, the preparation of samples takes a lot of time and there are few library spectra available, which makes it more difficult to identify and compare samples. However, Raman spectroscopy is an excellent technique for studying knee joint tissue calcification, since it can be used to study the articular cartilage, meniscus, and synovial fluid.

4.3. Other spectroscopic imaging techniques

Other spectroscopic imaging techniques that have been used to study calcifications in the knee joint are nuclear magnetic resonance (NMR), energy-dispersive X-ray spectroscopy (EDS), X-ray diffraction analysis (XRD), X-ray fluorescence (XRF) and X-ray absorption near edge structure (XANES).

NMR is used for example for chemical analysis and the determination of the sample's molecular structure. It is based on magnetic nucleus interactions with an external magnetic field. In NMR

spectroscopy the sample absorbs and emits nonionizing radiation at radio frequencies. The method is non-invasive, and it can be used in both liquid and solid-state samples.

EDS detects the X-rays that are released when an electron beam hits the sample and atoms shift from a higher energy state to a lower. EDS can be used for qualitative and quantitative analysis, enabling the user to identify both types of elements and the percentage of each element's concentration within the sample. EDS requires little to no sample preparation and is non-destructive. For even better results EDS is often coupled with a scanning electron microscope (SEM).

XRD is a diffraction-based technique for analyzing the atomic or molecular structure of materials. An X-ray analyzer is used to collect the x-rays diffracted from the sample forming a diffractogram that is unique for every sample It is non-destructive and works best with crystalline materials since x-rays scatter from regular arrays of atoms and molecules. An X-ray analyzer is used to collect the diffracted x-rays forming a diffractogram that is unique for every sample.

XRF is a technique used to measure the fluorescent that occurs when atoms in the sample emit X-rays or gamma-rays from the source. This technique can be used to determine the elemental and chemical composition of materials. XRF is non-destructive and needs only a little sample preparation.

XANES is a spectroscopic technique that enables the study of individual atoms from deep to superficial layers of the sample. A XANES spectrum is generated by measuring the fluorescence emission following X-ray absorption at a particular wavelength. The method is very sensitive to the identification of different elements. Nevertheless, the technique can only be used by laboratories with synchrotron, since the operation requires an intense source of X-ray radiation, which wavelength can be altered.

5. Spectroscopic studies on detecting calcification from knee joint tissues

A systematic review was carried out in order to find out the studies on detecting calcifications using spectroscopic methods in the meniscus, AC and SF. The following keywords were used in the 'PubMed' electronic database for searching the relevant articles on the meniscus, AC, and SF, respectively: [("Meniscus" AND "spectroscopy") AND "calcification"], [("Articular cartilage" AND "spectroscopy") AND "calcification"], and [("Synovial fluid" AND "spectroscopy") AND

"calcification"]. The search results were limited to English-language articles. The database was searched from commencement to 23 February 2022.

In beginning, a total of 83 articles were collected from the PubMed database. Among those 2 studies on the meniscus, 59 studies on AC, and 22 studies on SF. Among these studies, based on the following exclusion criteria: (i) studies related to other soft tissues or tissue-engineered materials; (ii) studies that had not used any spectroscopic methods for detection or characterization of calcifications; (iii) articles published in conference proceedings; (iv) studies with no originality; (v) studies comprising of the same dataset; (vi) review articles, only 12 studies were included. They are presented in the following tables 2,3 and 4.

Table 2: Characteristics of spectroscopic studies for the detection or characterization of calcification in the meniscus

Author/Year	Aims	Sample origin	Imaging/detecting methods	Comments
Dessombz A et al., 2013[14]	Analyze the structure of a trace element, Zn, present in the cartilage and meniscus of OA patients	Menisci and knee joint cartilage from end-stage OA patients	1. µXRF, µXANES, µXRD 2. FTIR	µXRD and FTIR identified CPPD. With µXRF spatial distribution of Ca and Zn were created for samples used. µXANES identified the Zn species.
Wang P et al.,2018[15]	To gain a way of grading the meniscus degeneration process at the molecular level	61 lyophilized human menisci from patients with different grades of degeneration.	IR-ATR spectroscopy	IR-ATR spectra of the meniscus provide molecular information on structural changes of cartilage at different stages of OA. Grade 1, grade 4, and grade 4 with calcification were separated based on their spectra.

Table 3: Characteristics of spectroscopic studies for the detection or characterization of calcification in articular cartilage

Author/Year	Aims	Sample origin	Imaging/detecting methods	Comments
Nguyen C et al., 2013[16]	Analyze the distribution of Calcium-containing crystals (CaC) in human knee OA cartilage and their biochemical and morphologic characteristics	142 knee joint cartilage samples from 20 end-stage OA patients	1. FTIR 2. SEM	FTIR detected CaC crystals in specimens for all patients. SEM detected the type of CaC crystals. BCPs were present in all samples but CPP was found in only 40%.
Cheung HS et al., 1996[17]	To study the effect of citrate, PC, and n-sulfo-2-amino-tricarballylate (SAT) on the ATP-induced CPPD crystal formation in both articular cartilage vesicles and native models.	Pig articular cartilage from the femoral condyles and patellae	1. IR 2. Chemical analysis 3. CPLM 4. Electron beam diffraction analysis	Crystals that resemble CPPD crystals were found together with IR, chemical analysis, and CPLM. The formation of the CPPD was confirmed with electron beam diffraction studies.
Fuerst M et al., 2010[18]	Develop a quantitative and identifying algorithm for cartilage mineralization in an experimental setting.	Articular cartilage from the knee of 4 OA patients	1. DCR 2. FESEM 3. X-ray element analysis 4. Raman spectroscopy	Despite Raman's ability to analyze samples at a micrometer scale, mineralization can be missed because it is not an accurate tool for excluding mineralization. Raman didn't detect BCP spectra during this research.

Table 4: Characteristics of spectroscopic studies for the detection or characterization of calcification in synovial fluid

Author/Year	Aims	Sample origin	Imaging/detecting methods	Comments
Frallonardo P et al., 2016[19]	To investigate the presence of CPP and BCP crystal in SF	74 knee OA patients	1. SEM coupled to EDS 2. Optical microscopy (CPLM for CPP, alizarin red staining for BCP)	Identification accuracy of CPP was similar with both CPLM (identified 24/74 OA SF samples) and SEM (identified 23/74 OA SF samples). However, there were 18 false-positive with SEM when identifying BCP. Thus, the SEM with EDS was more accurate when identifying different crystal types from SF.
Swan AJ et al., 1992[20]	To investigate the presence of CPP and BCP crystal in SF	11 knee OA, 5 RA, and 2 Pseudogout patients	1. AEM 2. XRD spectroscopy	CPPD crystals were found in 5 samples with AEM and 3 samples with XRD. BCP crystals were found in 8 with AEM and 5 with XRD. Light microscopy (AEM) gave false-positive results.
Valueva AV et al., 2020[21]	To evaluate the composition of phosphorus compounds in the synovial fluid	Knee joint fluid from patients with signs of CPPD	NMR spectroscopy	No detection of CPPD or BCP crystals was performed.
Bulysheva AA et al., 2018[22]	To study bone-derived crystal formation	SF: 4 donors	1. SEM with EDS 2. Raman spectroscopy	Raman analysis showed that bone in lactic acid had only CPPD crystals and no BCP crystals.
Cheng X et al., 2009[23]	To determine the minimum detectable crystal concentration by Raman analysis for MSUM and CPPD crystals and compare it with PLM	SF from donors	1. Raman spectroscopy and 2. PLM	Raman analysis has more detection limit of MSUM and CPPD crystals than PLM and was able to measure the amount of crystal.
Rosenthal AK et al., 2008[24]	To find out if sFTIR can be used to characterize and identify calcium-containing crystals	5 human knee joint fluids containing CPPD, 2 without CPPD but with OA	Synchrotron FTIR (sFTIR)	Accurate Identification of CPPD and BCP crystals was successful using sFTIR even with small and sparse calcium-containing crystals in a small amount of SF sample.
Li B et al., 2018[25]	Characterize the chemical composition of maltese cross birefringent (MCB)	174 SF samples from joint with symptoms	1. PLM, 2. Alizarin red S straining 3. Raman microspectroscopy, 4. SEM with EDS	CPLM detected 5,7 % of MCB in samples. Raman and SEM/EDS didn't detect BCPc nor phospholipids but rather suggested that MCB crystals are composed of calcium carbonates.

6. Characterization of the calcification types in the human menisci using Raman microspectroscopy

This section presents a Raman spectroscopic experiment to characterize the calcification types in the posterior horn of human menisci in total knee replacement (TKR) patients. For this experiment, high-resolution micro-computed tomography (µCT) images were used as a reference for identifying menisci with and without calcifications. A total of 40 meniscus posterior horn samples (both medial and lateral) were obtained from medial compartment knee OA patients (N=10, age [mean ± standard deviation]: 63±7, 50 % women, BMI: 28.7±3.5) undergoing TKR and cadaveric donors (N=10, age: 51±17, 50 % women, BMI: 28±6.9) without known knee OA. One subsection from every sample was fixed (formalin), dehydrated (ascending ethanol concentrations), hexamethyldisilazane (HMDS)-treated, air-dried, and imaged with a Bruker SkyScan 1272 µCT (50 kV, 200 µA, 2.0 µm pixel size, 2100 ms exposure time, 2400 projections, Al 0.25 mm filter). Adjacent to the µCT-subsection, a 5 µm thick tissue section was obtained and

placed on top of highly polished stainless-steel windows for Raman microspectroscopy. A Thermo Scientific™ DXR™2xi Raman imaging microscope, equipped with a 10×/0.25NA air objective and wide range grating (50-3250 cm^{-1} with a spectral resolution of 5 cm^{-1}), was used for Raman spectral acquisition. A 785 nm laser (28 mW) was used to excite the Raman signal and the spectra were collected for 0.5 s and averaged 5 times. Using the optical microscope of the Raman instrument, the calcifications could only be located on the tissue sections having severe calcifications. Hence, µCT images from the corresponding samples were used as a reference for selecting the regions of interest, and multiple Raman spectral maps from a tissue section were collected with a step size of 15 µm. The collected spectra were subjected to standard Raman spectral preprocessing. Chemical maps for both BCP and CPPD crystals were created by calculating the area under the 930-980 cm^{-1} band and 1020-1070 cm^{-1} band, respectively.

In the tissue sections of TKR patients, using Raman chemical maps, spectra of only triclinic calcium pyrophosphate dihydrate (t- CPPD, $Ca_2P_2O_7 \cdot 2H_2O$) were detected (a total of 69 820 Raman spectra) (Fig. 7). No Raman spectrum of BCP crystal was found in the analyzed tissue sections.

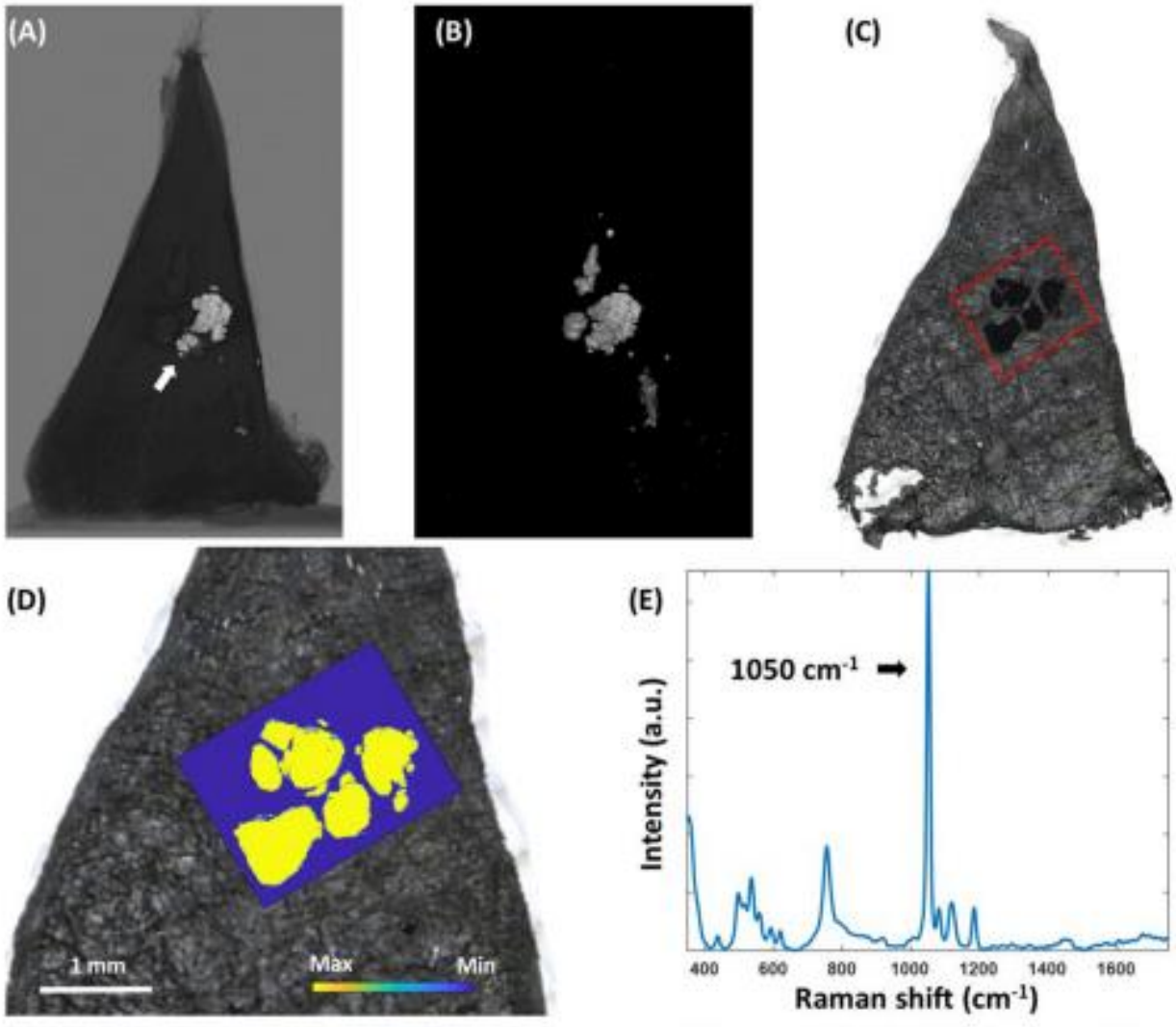

Fig 7: (A) An example of 3D micro-computed tomography (µCT) image of the meniscus posterior horn piece, calcified tissues pointed out with the white arrow. (B) Calcified tissues were visualized from 3D µCT images. (C) Optical microscopic view of the adjacent tissue section, the red box surrounding calcified tissues indicates the area to be scanned. (D) Raman chemical map of the 1020-1050cm^{-1} band, showing the distribution of calcium pyrophosphate dihydrate (CPPD) crystals inside the marked area after the scan. (E) Raman spectrum having the dominating 1050cm^{-1} peak confirms the presence of triclinic CPPD.

7. Summary

This thesis systemically reviews spectroscopic methods for detecting calcifications in the meniscus, articular cartilage, and synovial fluid in the knee joint. Moreover, the calcifications in the menisci of TKR patients have been characterized using Raman spectroscopy.

These most commonly known crystal types that form calcification in knee joints are CPPD and BCP. According to the systematic search, there are only a few studies in which meniscus calcification has been characterized. Spectroscopic methods that have been used to study the meniscus are µXRF, µXANES, µXRD, FTIR, and IR-ATR. In these studies, CPPD was identified using µXRD and FTIR.

The Raman spectroscopic experiment, presented here, showed that the calcifications in the meniscus posterior horns of TKR patients are mainly induced by CPPD deposition.

Compared to the meniscus, calcifications in articular cartilage have been studied extensively. µXRD and especially vibrational spectroscopy have been successfully used for the identification of the crystals in multiple studies. For example, Fuerst et al. 2010[17] reported that CPPD and HA can be found in cartilage affected by OA using Raman spectroscopy and verified the findings using SEM.

Finally, crystals in SF were also identified and characterized with XRD, FTIR, and Raman spectroscopy. In most of the studies, SEM coupled with EDS was used to verify the spectroscopic findings.

In conclusion, this thesis shows that spectroscopic methods, especially vibrational spectroscopies are very promising approaches for detecting and characterizing calcifications in soft tissues, as well as in synovial fluids. Calcifications in the knee joint could be a potential target for disease-modifying agents in OA therapy, and these spectroscopic techniques are vital tools for studying the calcifications in OA progression.

8. References

1. Dessombz A, Nguyen C, Ea HK, et al. Combining µX-ray fluorescence, µXANES and µXRD to shed light on Zn2+ cations in cartilage and meniscus calcifications. *Journal of Trace Elements in Medicine and Biology*. 2013;27(4):326-333. doi:10.1016/j.jtemb.2013.02.001
2. Sun Y, Mauerhan DR. Meniscal calcification, pathogenesis and implications. *Current Opinion in Rheumatology*. 2012;24(2):152-157. doi:10.1097/BOR.0b013e32834e90c1
3. Yavorskyy A, Hernandez-Santana A, McCarthy G, McMahon G. Detection of calcium phosphate crystals in the joint fluid of patients with osteoarthritis - Analytical approaches and challenges. *Analyst*. 2008;133(3):302-318. doi:10.1039/b716791a
4. Blewis ME, Nugent-Derfus GE, Schmidt TA, Schumacher BL, Sah RL. A model of synovial fluid lubricant composition in normal and injured joints. *European Cells and Materials*. 2007;13:26-38. doi:10.22203/ecm.v013a03
5. Bennike T, Ayturk U, Haslauer CM, et al. A normative study of the synovial fluid proteome from healthy porcine knee joints. *Journal of Proteome Research*. 2014;13(10):4377-4387. doi:10.1021/pr500587x
6. Sophia Fox AJ, Bedi A, Rodeo SA. The basic science of articular cartilage: Structure, composition, and function. *Sports Health*. 2009;1(6):461-468. doi:10.1177/1941738109350438
7. Chen S, Fu P, Wu H, Pei M. Meniscus, articular cartilage and nucleus pulposus: a comparative review of cartilage-like tissues in anatomy, development and function. *Cell and Tissue Research*. 2017;370(1):53-70. doi:10.1007/s00441-017-2613-0

8. Fox AJS, Bedi A, Rodeo SA. The Basic Science of Human Knee Menisci: Structure, Composition, and Function. *Sports Health*. 2012;4(4):340-351. doi:10.1177/1941738111429419

9. Petersen, W., Tillmann, B. Collagenous fibril texture of the human knee joint menisci. *Anat Embryol* 197, 317–324 (1998). https://doi.org/10.1007/s004290050141

10. Messner K, Gao J. *The Menisci of the Knee Joint. Anatomical and Functional Characteristics, and a Rationale for Clinical Treatment*. Vol 193.; 1998.

11. Berthomieu C, Hienerwadel R. Fourier transform infrared (FTIR) spectroscopy. *Photosynthesis Research*. 2009;101(2-3):157-170. doi:10.1007/s11120-009-9439-x

12. Turunen M. *Spectroscopic Characterization of Bone Composition Alterations during Bone Formation, Maturation and Aging*. http://www.uef.fi/kirjasto

13. Lagos M, Paredes R, Retamal C. Fourier Transform Spectrometry with Fourier Analysis of the Interferogram as Just an Optional Tool. *ACS Omega*. 2018;3(12):18258-18262. doi:10.1021/acsomega.8b02914

14. Dessombz A, Nguyen C, Ea HK, et al. Combining µX-ray fluorescence, µXANES and µXRD to shed light on Zn2+ cations in cartilage and meniscus calcifications. *Journal of Trace Elements in Medicine and Biology*. 2013;27(4):326-333. doi:10.1016/j.jtemb.2013.02.001

15. Wang P, Balko J, Lu R, López-Lorente ÁI, Dürselen L, Mizaikoff B. Analysis of human menisci degeneration: Via infrared attenuated total reflection spectroscopy. *Analyst*. 2018;143(20):5023-5029. doi:10.1039/c8an00924d

16. Nguyen C, Bazin D, Daudon M, et al. Revisiting spatial distribution and biochemical composition of calcium-containing crystals in human osteoarthritic articular cartilage. *Arthritis Research and Therapy*. 2013;15(5). doi:10.1186/ar4283

17. Cheung HS, Kurup I v, Sallis JD, Ryan LM. *Inhibition of Calcium Pyrophosphate Dihydrate Crystal Formation in Articular Cartilage Vesicles and Cartilage by Phosphocitrate**.; 1996. http://www-jbc.stanford.edu/jbc/

18. Fuerst M, Lammers L, Schäfer F, et al. Investigation of calcium crystals in OA knees. *Rheumatology International*. 2010;30(5):623-631. doi:10.1007/s00296-009-1032-2

19. Frallonardo P, Oliviero F, Peruzzo L, et al. Detection of Calcium Crystals in Knee Osteoarthritis Synovial Fluid: A Comparison between Polarized Light and Scanning Electron Microscopy. *Journal of Clinical Rheumatology*. 2016;22(7):369-371. doi:10.1097/RHU.0000000000000416

20. Swan A, Chapman B, Heap P, Seward H, Dieppe P. Submicroscopic crystals in osteoarthritic synovial fluids. *Annals of the Rheumatic Diseases*. 1994;53(7):467-470. doi:10.1136/ard.53.7.467

21. Valueva A v., Romanov RS, Mariasina SS, Eliseev MS, Rodina E v. Inorganic Pyrophosphatase-Nanodiamond Conjugates Hydrolyze Pyrophosphate in Human Synovial Fluid. *ACS Omega*. 2020;5(15):8579-8586. doi:10.1021/acsomega.9b04429

22. Bulysheva AA, Sori N, Francis MP. Direct crystal formation from micronized bone and lactic acid: The writing on the wall for calcium-containing crystal pathogenesis in osteoarthritis? *PLoS ONE*. 2018;13(11). doi:10.1371/journal.pone.0202373

23. Cheng X, Haggins DG, York RH, Yeni YN, Akkus O. Analysis of Crystals Leading to Joint Arthropathies by Raman Spectroscopy: Comparison with Compensated Polarized Imaging. *Applied Spectroscopy*. 2009;63(4):381-386. doi:10.1366/000370209787944280

24. Rosenthal AK, Mattson E, Gohr CM, Hirschmugl CJ. Characterization of articular calcium-containing crystals by synchrotron FTIR. *Osteoarthritis and Cartilage*. 2008;16(11):1395-1402. doi:10.1016/j.joca.2008.03.019

25. Li B, Singer N, Rosenthal A, et al. Chemical characterization of Maltese-cross birefringent particles in synovial fluid samples collected from symptomatic joints. *Joint Bone Spine*. 2018;85(4):501-503. doi:10.1016/j.jbspin.2017.09.004